

Gravity field over the Sea of Galilee: Evidence for a composite basin along a transform fault

Zvi Ben-Avraham,¹ Uri ten Brink,² Robin Bell,³ and Margaret Reznikov^{1,4}

Abstract. The Sea of Galilee (Lake Kinneret) is located at the northern portion of the Kinneret-Bet Shean basin, in the northern Dead Sea transform. Three hundred kilometers of continuous marine gravity data were collected in the lake and integrated with land gravity data to a distance of more than 20 km around the lake. Analyses of the gravity data resulted in a free-air anomaly map, a variable density Bouguer anomaly map, and a horizontal first derivative map of the Bouguer anomaly. These maps, together with gravity models of profiles across the lake and the area south of it, were used to infer the geometry of the basins in this region and the main faults of the transform system. The Sea of Galilee can be divided into two units. The southern half is a pull-apart that extends to the Kinarot Valley, south of the lake, whereas the northern half was formed by rotational opening and transverse normal faults. The deepest part of the basinal area is located well south of the deepest bathymetric depression. This implies that the northeastern part of the lake, where the bathymetry is the deepest, is a young feature that is actively subsiding now. The pull-apart basin is almost symmetrical in the southern part of the lake and in the Kinarot Valley south of the lake. This suggests that the basin here is bounded by strike-slip faults on both sides. The eastern boundary fault extends to the northern part of the lake, while the western fault does not cross the northern part. The main factor controlling the structural complexity of this area is the interaction of the Dead Sea transform with a subperpendicular fault system and rotated blocks.

Introduction

The Sea of Galilee (Lake Kinneret) is located at the northern portion of the Kinneret-Bet Shean basin (Figure 1a), in the northern Dead Sea rift [Schulman, 1962; Freund, 1978]. The Dead Sea rift is a plate boundary of the transform type which connects the Red Sea, where seafloor spreading occurs, with the Zagros zone of continental collision [Freund, 1965; Garfunkel, 1981]. The Dead Sea transform follows a small circle from its southern edge at the northern Red Sea to the Sea of Galilee area [Garfunkel, 1981]. North of the Hula basin the main trace of the transform changes its orientation to the northeast (Figure 1b) and forms the Yammuneh fault, while other faults, mainly the Roum fault in Lebanon, continue along the small circle to the continental margin near Beirut [Girdler, 1990]. At the region occupied by the Kinneret-Bet Shean basin a secondary NW-SE to W-E trending fault system, which is composed of branching faults, exists on the western side of the transform fault (Figure 1b). Farther north, branching faults were developed on the other side of the transform fault in the Palmyra Range area [Walley, 1988]. A diffusion of slip from the main transform takes place along the branching faults as the Arabian and African Plates approach the collision

zone at the Alpine orogenic belt [Ben-Menahem *et al.*, 1976; Nur and Ben-Avraham, 1978].

The structure of the Kinneret basin appears to be more complex than that of other pull-apart basins along the Dead Sea transform (e.g., Dead Sea basin, Hula basin). The complexity of the area results from the fact that two fault systems intersect in the lake's area. The main fault system trends north-south and is part of the Dead Sea transform, and the secondary fault system trends NW-SE on the western side of the main fault and extends into the Galilee. Superposition of vertical displacements perpendicular or oblique to the transform created complicated structures in this area. Because Plio-Pleistocene basalt flows and intrusions of variable thickness cover the area [Neev, 1978; Mor, 1986], structural interpretation of the Kinneret-Bet Shean basin is difficult.

The geometry of the plate boundary in the Sea of Galilee area has been the subject of considerable debate [Freund, 1978; Garfunkel, 1981; Kashai and Croker, 1987; Rotstein and Bartov, 1989; Rotstein *et al.*, 1992; Heimann and Ron, 1993]. The main problems in depicting the geometry of the plate boundary resulted from the lack of geophysical data from the Sea of Galilee and the lack of surface expressions of faults in the northern Sea of Galilee and in the area north of the lake.

The Sea of Galilee is a body of freshwater whose surface is at about 210 m below mean sea level (msl). Its length is about 20 km, its maximum width is about 12 km, and its maximum depth is 46 m (Figure 2). The Kinarot Valley south of the lake is a narrow rift valley; the valley floor dips gently southward. North of the Sea of Galilee is the Korazim Heights, an elevated feature which is intensely deformed and covered mostly by basalts [Heimann and Ron, 1993]. Farther north, another pull-apart basin exists beneath the Hula Valley [Garfunkel, 1981].

Previous studies of the subbottom structure of the lake have

¹Department of Geophysics and Planetary Sciences, Tel Aviv University, Tel Aviv, Israel.

²U.S. Geological Survey, Woods Hole, Massachusetts.

³Lamont-Doherty Earth Observatory, Palisades, New York.

⁴Now at the Institute for Petroleum Research and Geophysics, Holon, Israel.

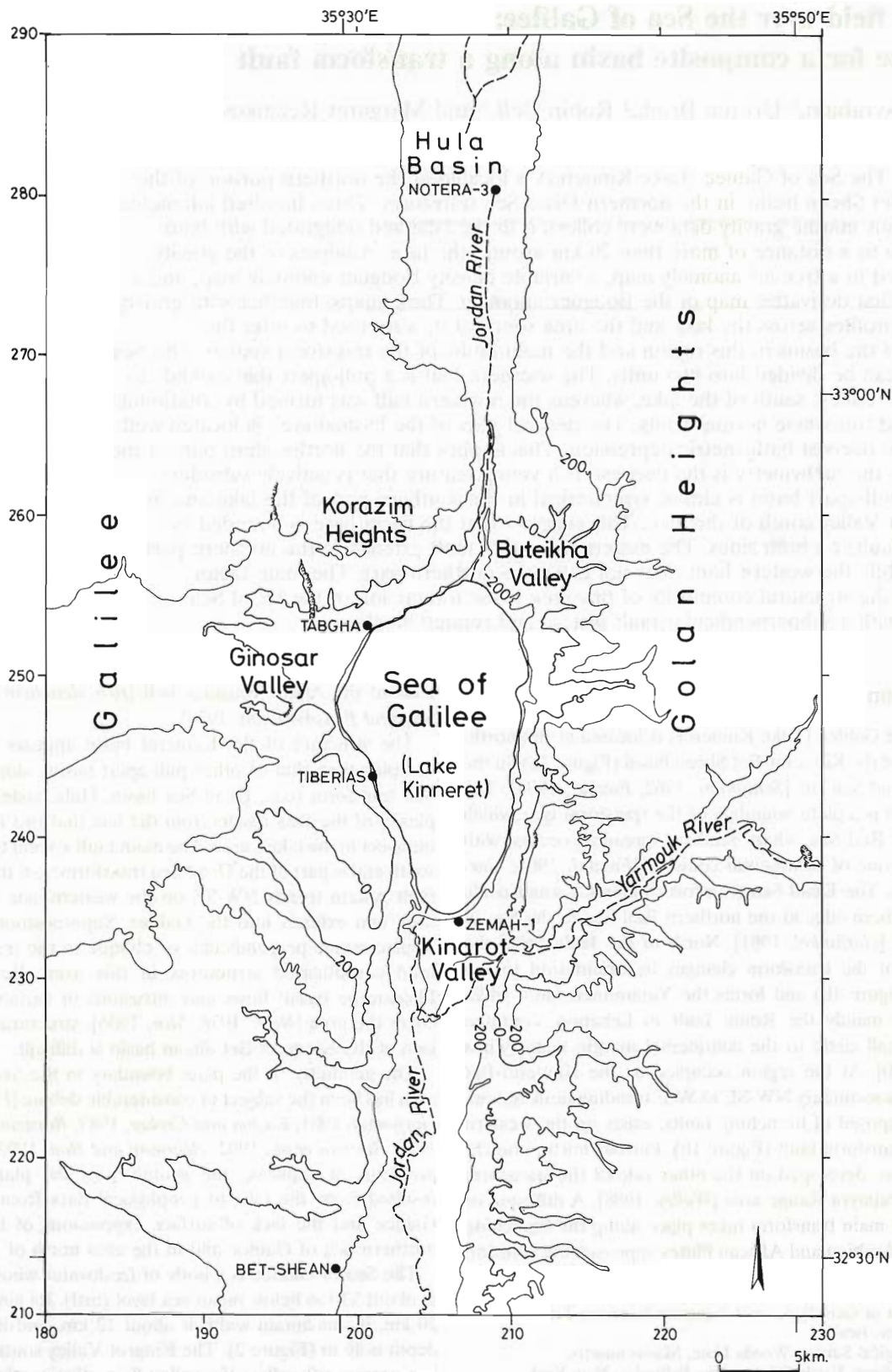


Figure 1a. Location map of the Sea of Galilee and its vicinity. Topographic contours 200, 0, and -200 m are shown. The locations of Zemah 1 and Notera 3 wells are also shown. The Kinneret-Bet Shean basin extends from the northern shore of the Sea of Galilee in the north to latitude 32°28'N in the south. Both geographic and Israeli coordinate system are shown.

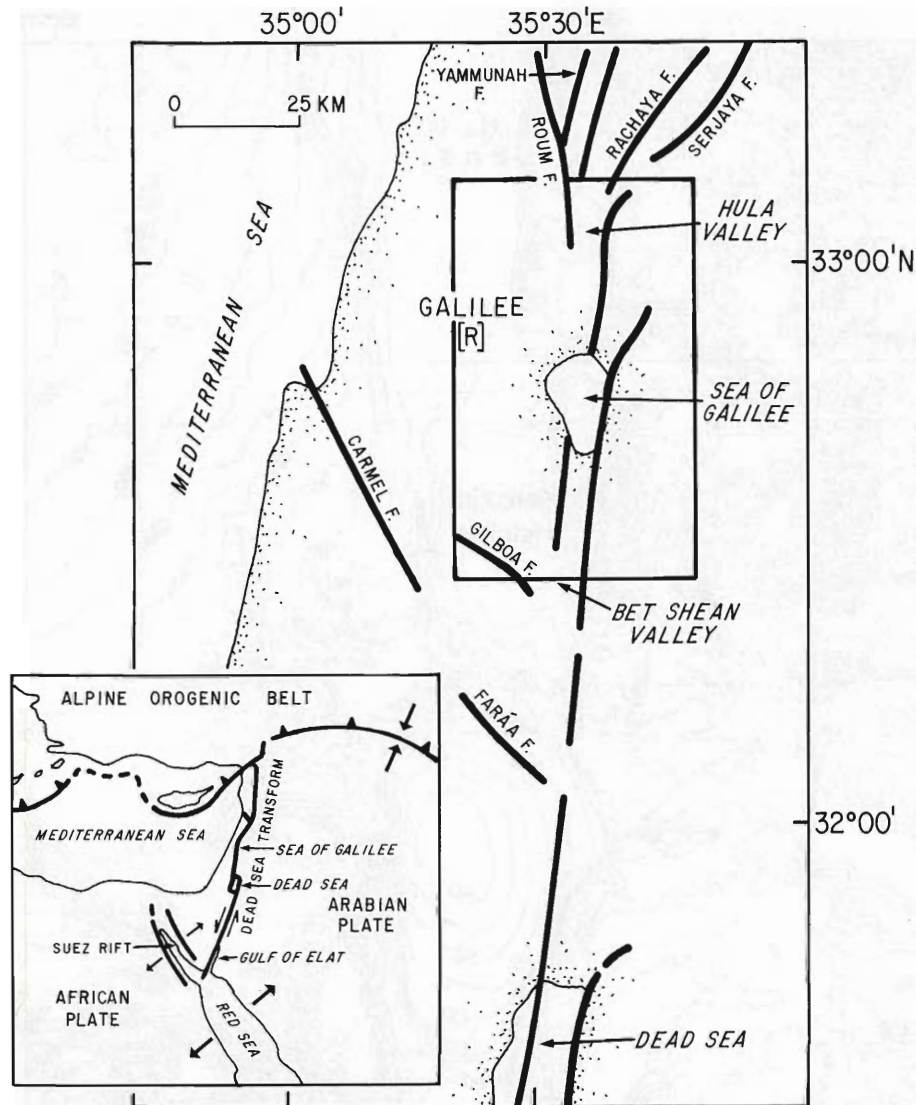


Figure 1b. Major faults of the Dead Sea transform system [after van Eck and Hofstetter, 1990; Heimann and Ron, 1993]. The box outlines the boundaries of the maps in Figures 1a–6 and 8. [R] marks the area of pervasive faulting accompanied by block rotation. Inset shows the configuration of tectonic plates.

used various methods including seismic reflection and refraction [Ben-Avraham et al., 1981, 1986], magnetics [Ben-Avraham et al., 1980; Ginzburg and Ben-Avraham, 1986], bathymetry [Ben-Avraham et al., 1990], and heat flow [Ben-Avraham et al., 1978]. Although the seismic reflection profiles in the Sea of Galilee are of poor quality, they indicate that the lake area is tectonically active. Active faults and folded structures were detected in the uppermost sediments along the margins and in the interior of the lake [Ben-Avraham et al., 1981]. The seismic reflection profiles were obtained with various instruments, all high-resolution single channel with maximum penetration of about 40 m. The maximum penetration of the seismic refraction profiles was 630 m.

Several seismic profiles were obtained north and south of the lake [Rotstein and Bartov, 1989; Rotstein et al., 1992]. A few holes were drilled in the vicinity of the lake; the deepest one is the Zemah 1 well located at the center of the Kinarot Valley, south of the lake. It penetrated a 4249-m sequence of graben fill consisting of clastic, evaporitic, and both intrusive and ex-

trusive igneous rocks [Marcus and Slager, 1985]. The valley is covered by the Quaternary Lisan Formation (Figure 3).

In order to learn more about the subbottom structure of the Sea of Galilee, we conducted in October 1988 a detailed gravity survey on the lake. The marine data were combined with gravity data on land around the lake to constrain the geometry and structure of the basin and understand its development.

Methods

Gravity measurements in the Sea of Galilee were made aboard R/V *Hermona*, a 6-m-long boat of the Kinneret Limnological Laboratory, Israel Oceanographic and Limnological Research Ltd., using a BGM-3 sea gravity meter of Lamont-Doherty Earth Observatory. Positions were obtained with a Motorola Miniranger navigation system.

The BGM-3 gravity meter system, manufactured by Bell Aerospace, consists of an inertial navigation-grade accelerometer mounted on a gyro-stabilized platform and a data handling

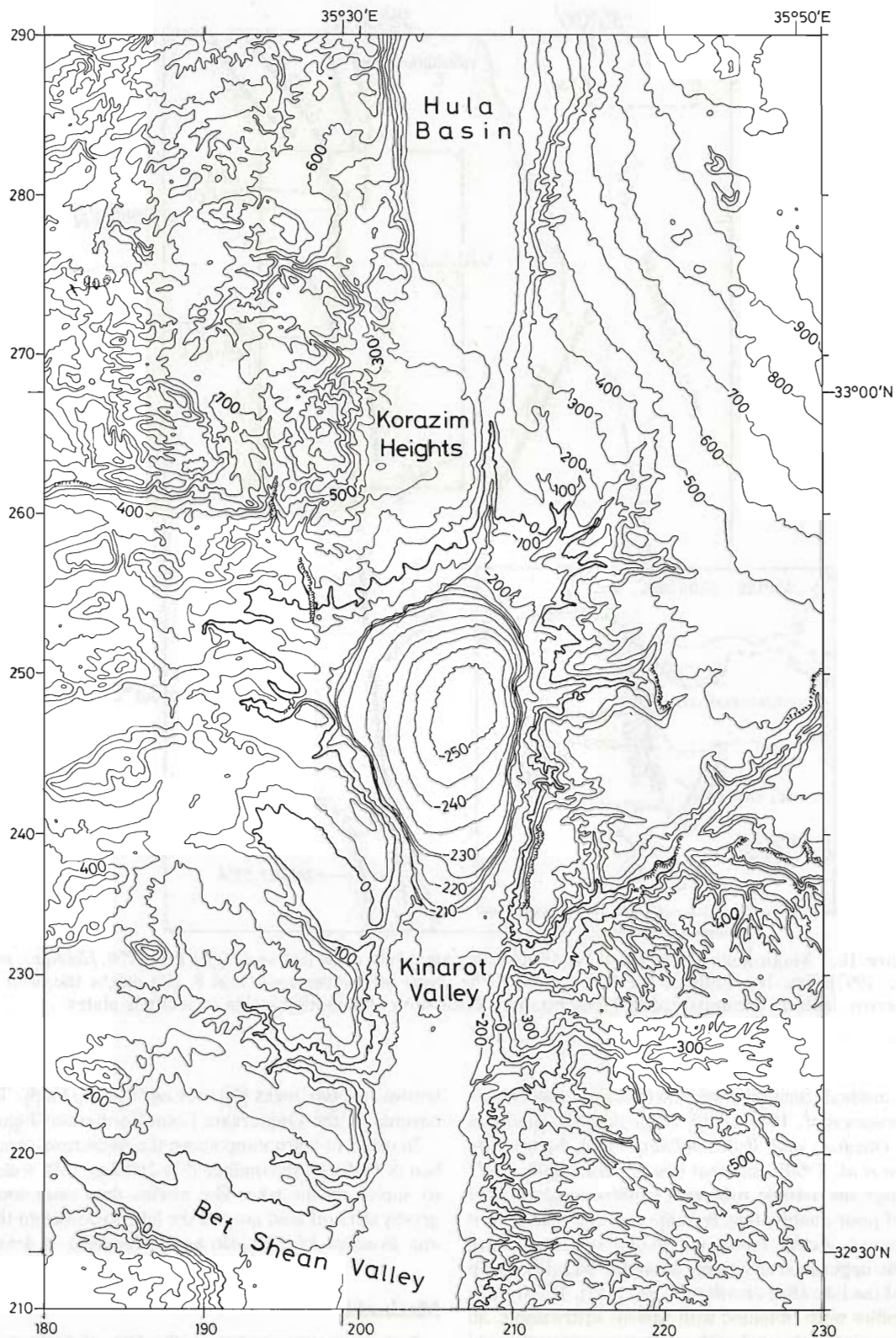


Figure 2. Simplified topographic map of the Sea of Galilee and its vicinity. Contour interval is 100 m on land and 10 m in the lake.

system [Bell and Watts, 1986]. The small size of the gravity meter system made it possible to use a relatively small boat for the measurements.

The measurements were made along a grid of east-west and

north-south lines spaced 1–2 km apart. The total length of lines was about 300 km. The gravity data were collected every 1 s and were averaged once a minute. Since the average speed of the boat was 10 knots (18.5 km/hour), about 1000 new grav-

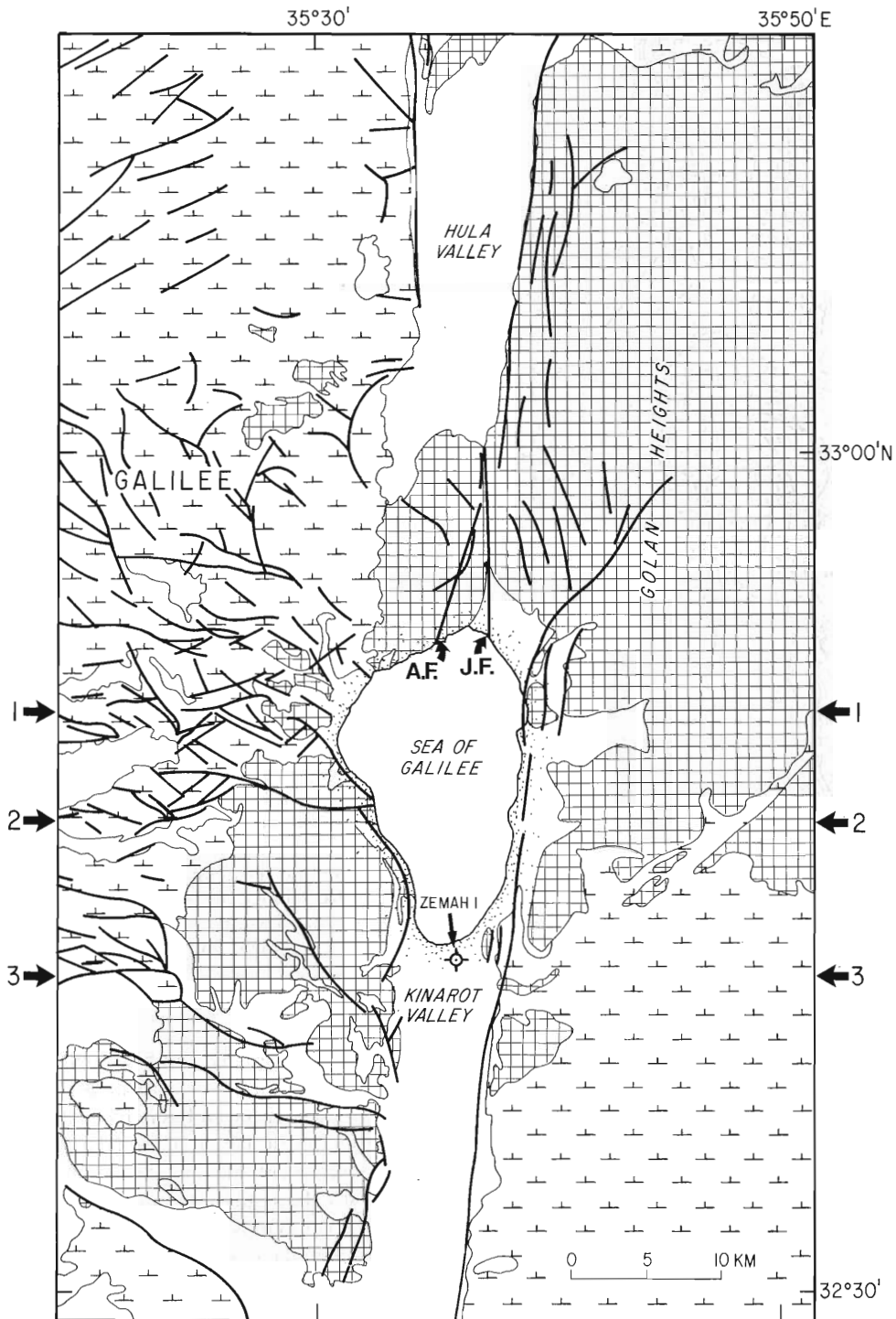


Figure 3. Simplified geological map of the land area surrounding the Sea of Galilee (modified from *Picard and Golani [1976]* and *Ron et al., [1984]*). The patterns are grid, Pliocene to Pleistocene basalts; inverted Ts, Jurassic-Eocene sediments (mainly carbonates); open areas, Neogene to recent clastic and lacustrine sediments of graben fill. Arrows indicate the locations of gravity profiles (Figure 7). The location of Zemah 1 drill hole is shown. Abbreviations are AF, Almagor fault [*Heimann and Ron, 1993*]; JF, Jordan fault.

ity measurements were collected, one every 300 m along the lines.

A moving average filter with a 200-s Gaussian window was applied to the gravity data to remove the accelerations of the boat. The data were manually edited to remove bad measurements. Eötvös correction was applied to compensate for the

boat's velocity. The uncertainty of the gravity measurement is less than 1.5 mGal, and the uncertainty of the navigation was estimated at about 3 m. Bathymetric data were available from an earlier survey [*Ben-Avraham et al., 1990*] in which measurements were made on a grid of east-west and north-south lines with line spacing of 100 m. An average of the bathymetric data

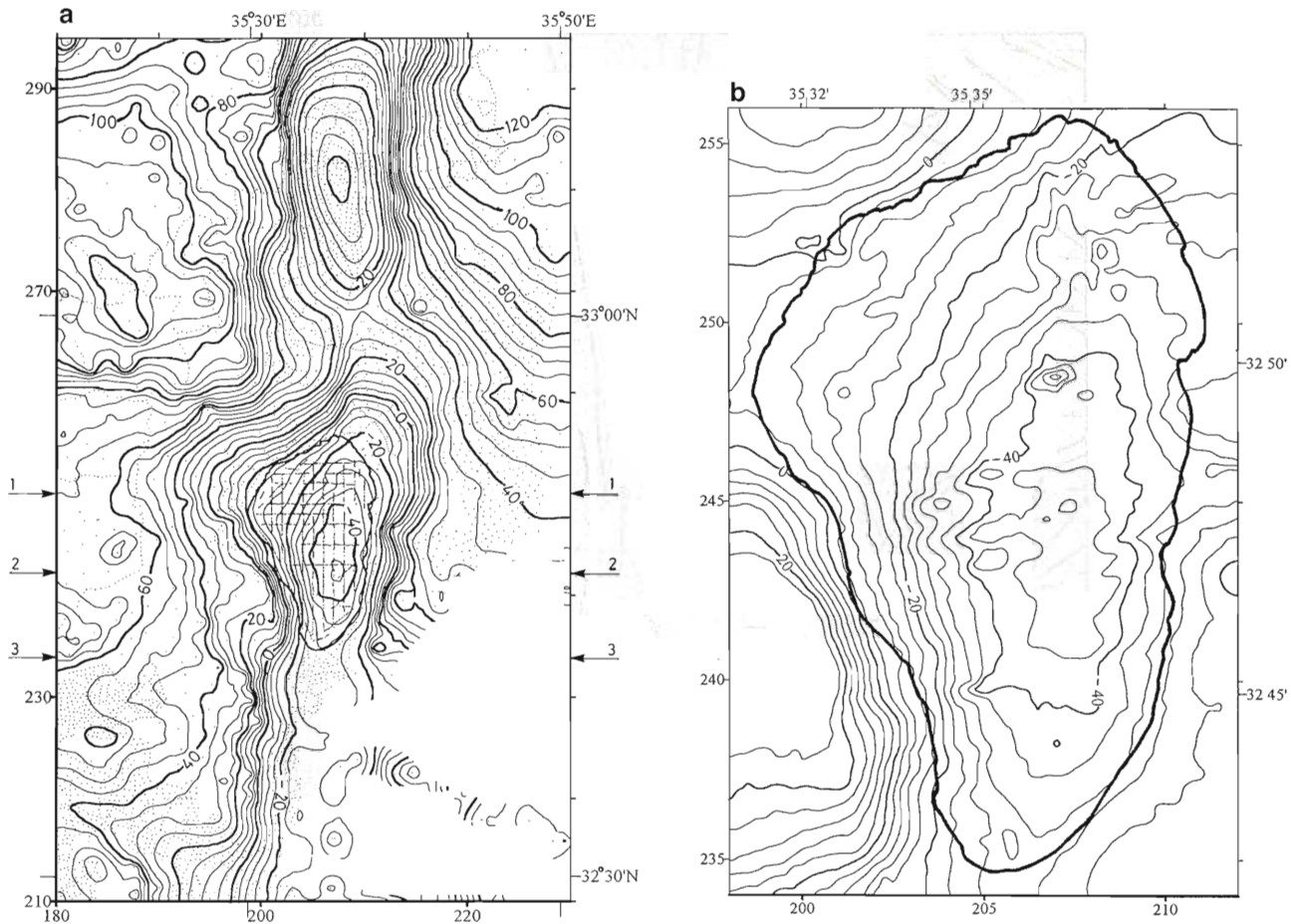


Figure 4. (a) Free-air gravity anomaly map of the Sea of Galilee and its vicinity and locations of gravity stations (dots on land and lines in the lake). The gravity values were gridded at 0.65-km square cell size and smoothed. Contour interval is 5 mGal. Arrows at the sides of the map indicate locations of gravity profiles (Figure 7). (b) Free-air gravity anomaly map of the Sea of Galilee. The gravity values were gridded at 0.2-km square cell size and smoothed. Contour interval is 4 mGal.

was computed within a circle with a radius of 25 m around every gravity measurement.

The gravity measurements over the Sea of Galilee were combined with gravity data in the surrounding areas which were obtained from the archives of the Institute of Petroleum Research and Geophysics, Israel. Relatively few data points exist east of the lake, while a dense coverage exists south, west, and north of the lake. The tie with land data was accomplished by repeated measurements at the Kinneret Limnological Laboratory dock and a known reference station of the Israeli gravity network. The land values were recalculated using the 1967 International Gravity Formula.

Free-Air and Bouguer Gravity Anomalies

The free-air gravity anomaly map (Figure 4a) shows many of the same features as the topography. The anomaly is quite variable: the lake coincides with a negative anomaly (-40 mGal) and the surrounding highlands with positive anomalies ($+120$ mGal). To the west the anomaly is rather flat and drops by about 100 mGal into the basin. The Kinneret-Bet Shean basin, the Korazim Heights north of it, and the Hula basin farther north are well defined lows on the map. Several zones of steep gradient of the gravity field can be observed in asso-

ciation with topographic and bathymetric escarpments. Steep gradients of 25 mGal/km exist in places along the western margin of the Bet Shean basin, including the Kinarot Valley, and the southwest margin of the lake.

An enlargement of the free-air anomaly within the lake (Figure 4b) shows that the gravity minimum, defined by the -40 -mGal contour, is displaced to the eastern side of the lake and is south of the principal bathymetric depression of the lake (compare with Figure 2). In the southern part of the lake a steep gradient in the free-air gravity anomalies is oriented north-south and is located between the western coastline and the gravity minimum. It extends about half way up the lake from the southern edge of the lake. The steepest topographic escarpment is, on the other hand, along the eastern side of the lake.

Following density measurements by Folkman [1976] and a gravity study of the Dead Sea basin [ten Brink *et al.*, 1993], two densities were chosen for the Bouguer corrections of Figure 5: 2550 kg/m^3 for all the points shallower than 150 meters below sea level (msl) and 2150 kg/m^3 for all the points deeper than 150 mbsl. The first density corresponds to the Mesozoic and early Cenozoic carbonate cover outside the transform valley and the second to the Quaternary sediments inside the valley.

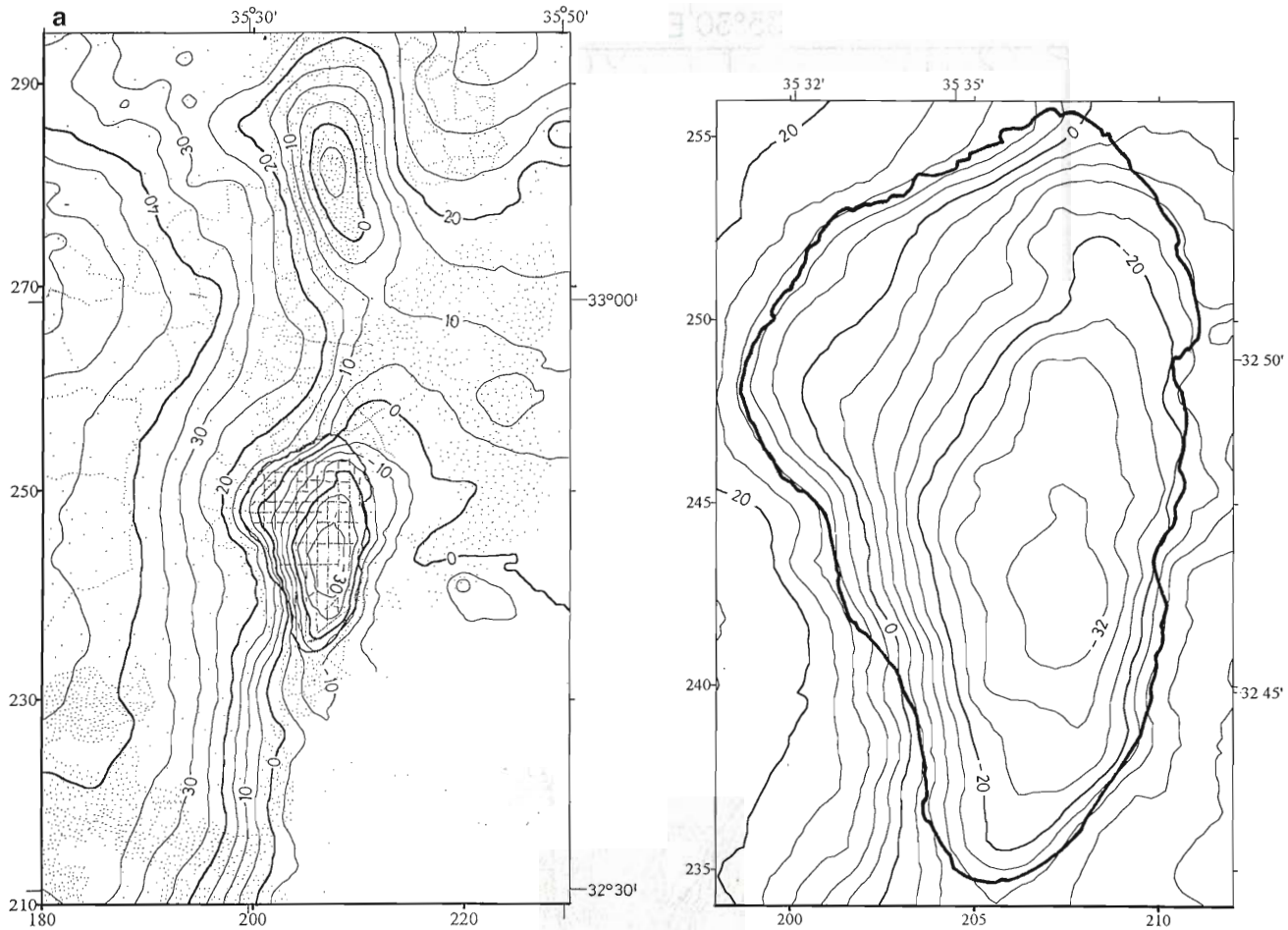


Figure 5. (a) Bouguer gravity anomaly map of the Sea of Galilee and its vicinity and locations of gravity stations (dots on land and lines in the lake). The gravity values were gridded at 0.65-km square cell size and smoothed. Density used for the Bouguer correction is 2550 kg/m³ above 150 meters below sea level (mbsl) and 2150 kg/m³ below 150 mbsl. Reference level for map and lake level during the experiment is 210.2 mbsl. Contour interval is 5 mGal. (b) Bouguer gravity anomaly map of the Sea of Galilee. The gravity values were gridded at 0.2-km square cell size and smoothed. Contour interval is 4 mGal.

The water density was replaced with a density of 2150 kg/m³. A reference level of -210.2 m (the lake level during the experiment) was chosen for the Bouguer correction.

Bouguer gravity correction is an effective way of removing the gravitational influence of local (short wavelength) topography. The Bouguer anomaly map (Figure 5a) shows the regional gradient which decreases to the east across the Dead Sea transform from values in excess of 40 mGal to values around 0 mGal. West of the Dead Sea transform, the Bouguer gravity map shows a gravity gradient decreasing eastward. A similar eastward gradient was observed farther south (along latitude 32°00'N) and was interpreted to represent thickening of the crust from ≤ 12 km in the Mediterranean Sea to 35 km in the Arabian Plate [ten Brink *et al.*, 1990]. The gradient is steepest close to the transform indicating possibly a step in Moho thickness across the transform, due to the juxtaposition of crusts of different thickness by the strike-slip motion [ten Brink *et al.*, 1990]. The gradient greatly reduces east of the transform, probably due to the fact that there is no thickening of the crust beyond the plate boundary. Two oblong-shaped areas of relatively negative gravity anomaly exist over the Sea of Galilee and the Hula basin.

Within the lake the Bouguer gravity minimum, denoted by

the -30-mGal contour, is located at about the same place as the free-air gravity minimum (Figure 5b). The northeastern margin of the lake is not well defined by the contours of either the free-air or Bouguer gravity anomalies.

The gravity maps (Figures 4 and 5) and first horizontal derivative map suggest that Sea of Galilee is divided into two subbasins. The center of the deepest one coincides within the gravity minimum at latitude 32°46'N, and it extends southward into the Kinarot Valley. It also extends northward up to the widest part of the lake, at latitude 32°50'N, and has an elongated shape in a north-south direction. The second more subtle E-W trending subbasin occupies the widest part of the lake. It may extend to the northeast into the Buteikha Valley on land and to the west into the Ginosar Valley on land.

The first horizontal derivative map of the Bouguer anomalies (Figure 6) emphasizes the short wavelength features of the Bouguer anomalies. The Kinneret-Bet Shean basin is bounded on the western side by a lineament of high gravity gradient. The crest of the maximum gradient in this area probably represents a fault separating rocks of different densities. Within the lake itself the western gradient widens and appears to split away from the southwest coast of the lake which is also associated with high gravity gradient. On the east a lineament of

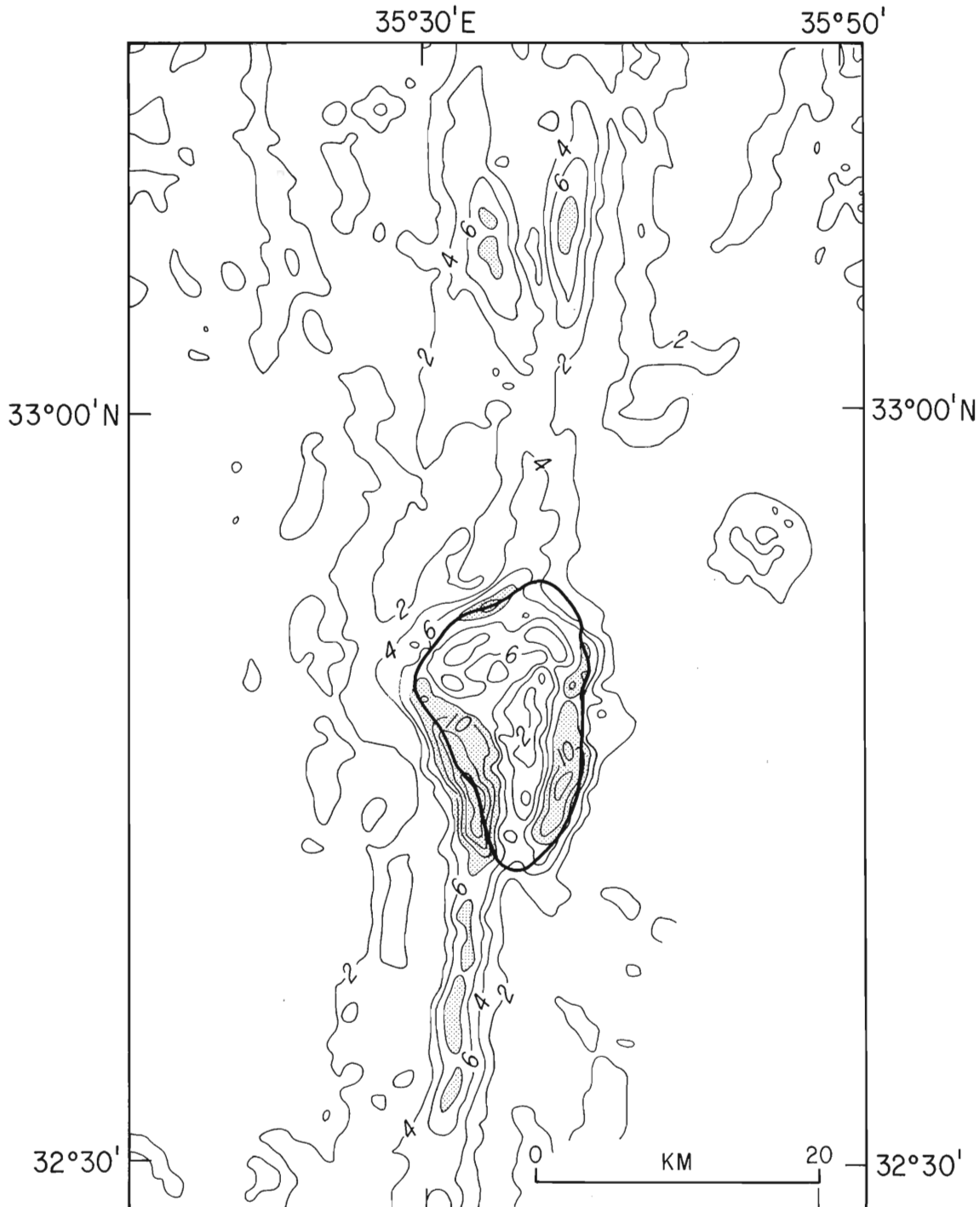


Figure 6. Map of the magnitude of the first horizontal derivative of the Bouguer anomaly map. Map emphasizes the short wavelength features of the Bouguer map (Figure 5). Contour interval is 2 mGal/km.

high gravity gradient borders the Sea of Galilee and the Kinarot Valley, south of the lake. It probably extends farther south; however, only one profile of gravity stations at $\sim 32^{\circ}35'N$ extends east of the valley. The Hula basin is bounded, like the southern Kinneret-Kinarot basin, on the eastern and western sides by lineaments of high gravity gradients. The first horizontal derivative map (Figure 6) also shows a high gravity gradient along the northwestern margin of the lake. This suggests that a subsurface fault probably separates the Korazim Heights from the Sea of Galilee basin.

Gravity Models

Three two-dimensional gravity models were calculated along east-west profiles across the basin and adjacent land areas and compared with free-air anomalies along the profiles (Figure 7). Two are located across the lake and one south of the lake (Figures 3 and 4). No gravity data exist east of the Kinarot Valley south of the lake along the eastern part of profile 3. Therefore data from the single profile of gravity stations located south of the profile at $\sim 32^{\circ}35'N$ and data from the area

north of it were interpolated to fill the gap. A linear trend was removed from the free-air gravity profiles prior to the modeling. The densities that were used are of Lake Kinneret water (1000 kg/m^3), the sediment fill (2150 kg/m^3), the Mesozoic-early Cenozoic carbonates (2550 kg/m^3), the crystalline basement (2670 kg/m^3), and the Tertiary basalt flows (2750 kg/m^3). The thickness of the basalt flows in the models ranges between 150 and 200 m in accordance with the observation of Mor [1986] on basalt flows in the Golan Heights.

The models used available geological and geophysical information including topography and bathymetry, seismic data [Ben-Avraham et al., 1981; Rotstein et al., 1992], stratigraphic information from the Zemah 1 well [Marcus and Slager, 1985], and the depth to crystalline basement [Ginzburg et al., 1979] along the west margin of the Dead Sea transform. The latter is unknown under the Kinneret-Bet Shean basin.

The models indicate that the width and depth of the basin vary along its length. The deepest part of the basin reaches more than 6 km. The width varies from 8 to 18 km. The models for the southern part of the lake (profile 2) and for the Kinarot Valley (profile 3) suggest that the narrow, deep basin in this region is probably bordered by faults on both sides. In the northern part of the lake the main basin extends westward toward the Ginosar Valley on land with reduced thickness of the sedimentary fill. In this part (profile 1), only the eastern side is probably bordered by a fault.

The Structure of the Sea of Galilee

The analysis of the gravity data together with previously obtained bathymetric, seismic, and magnetic data provides information about the structure of the Sea of Galilee. The lake can be divided into two distinct units. South of latitude $32^\circ 49' \text{N}$, the lake is narrow and bordered by two north-south trending boundary faults (Figures 6 and 7). In this area the basin is the deepest. North of latitude $32^\circ 49' \text{N}$, the basin is wider. The western boundary fault at the southern part of the lake probably does not continue into the northern part. The main basin in the southern part of the lake is shown as a valley in the first horizontal derivative map (Figure 6). It has an elongated shape, typical of pull-aparts. The western boundary at this part of the basin continues southward into the Kinarot and Bet Shean Valleys.

The floor of the lake is quite smooth probably because of the considerable sedimentation rate. A notable exception is a small WNW trending bathymetric scarp at water depths of 13–21 m along latitude $32^\circ 44' \text{N}$ (note the contours -225 m and -230 m in Figure 2). Seismic reflection and magnetic data suggest that the scarp is a surface expression of a fault [Ben-Avraham and ten Brink, 1989]. It could mark the location of a transverse fault that separates the Kinarot Valley from the southern part of the lake. However, this fault is not associated with a high gravity gradient.

The gravity models suggest that the basin in the southern part of the lake is a full graben or close to a full graben similar to the Dead Sea basin [ten Brink et al., 1993]. On the basis of earlier studies in the Gulf of Elat [Ben-Avraham, 1985] and other continental transforms [Ben-Avraham, 1992; Ben-Avraham and Zoback, 1992], this situation probably indicates that strike-slip motion is taking place along both the western and eastern boundary faults in the southern part of the lake (Figure 8). The western boundary fault in the deep part of the lake is expressed in the bathymetry [Ben-Avraham et al., 1990] as a step in the otherwise smooth slope of the lake floor.

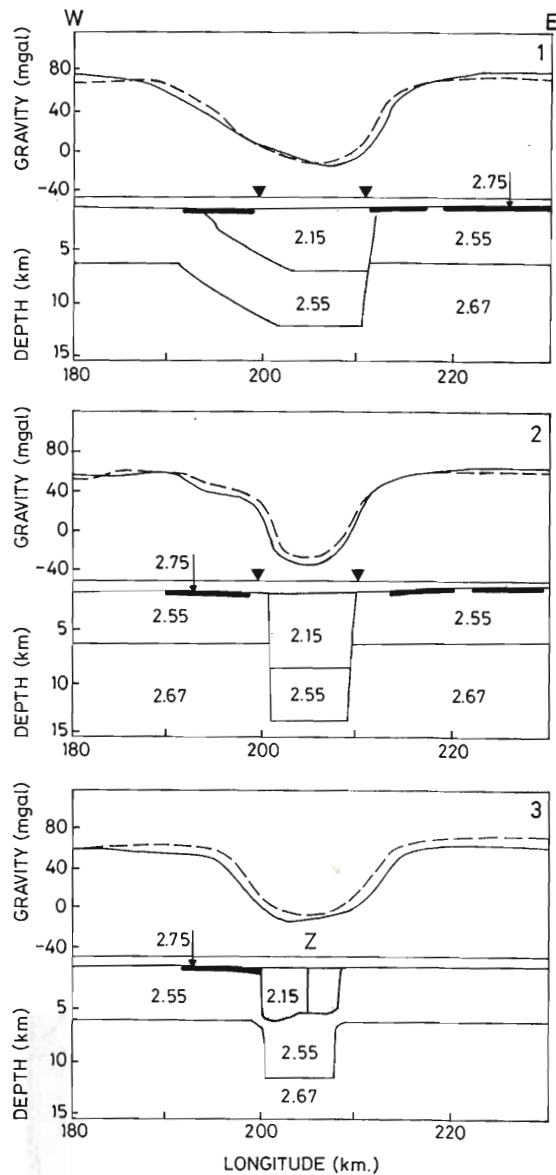


Figure 7. Three east-west gravity profiles (dashed lines, see Figures 3 and 4a for location) extracted from the gridded free-air gravity data shown in Figure 4 with linear trend removed, compared with calculated gravity (solid lines) from two-dimensional density-depth models (below the profiles). Density is $1 \times 10^3 \text{ kg/m}^3$. Values for the eastern part of profile 3 were interpolated from data north and south of it. Dark layers are basalt flows. Distance in kilometers is measured from longitude 180, Israel coordinate system. Location of Zemah 1 drill hole is shown on profile 3. Inverted triangles mark the boundaries of the lake.

Although the situation in the Kinarot Valley, south of the lake, is less clear because of the lack of gravity data east of the valley except for a single profile of gravity stations, evidence from seismic reflection profiles suggests that a full graben may also exist here. Rotstein et al. [1992] have proposed on the basis of high-resolution multichannel seismic profiles en echelon arrangements of the Dead Sea transform segments in the Kinarot Valley.

The Bouguer gravity map (Figure 5b) and the gravity models further suggest that the basin in the northern part of the lake is asymmetric to the east. However, strike-slip motion along

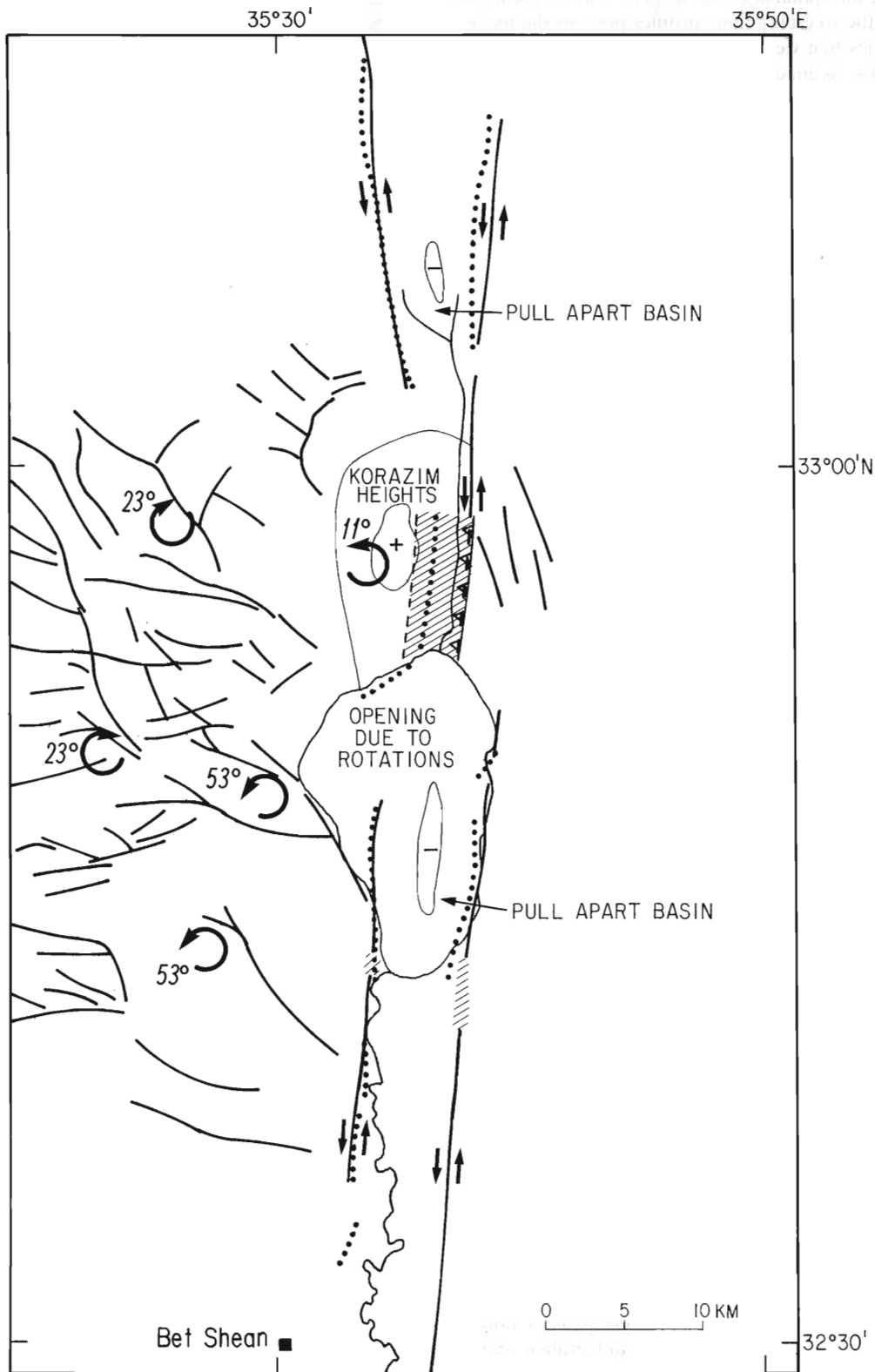


Figure 8. Schematic map showing the main structural elements in the Sea of Galilee and its vicinity. Heavy lines are faults. Faults with arrows mark our interpretation of strike-slip fault strands of the transform. The lows in the Sea of Galilee and Hula basin are from the first horizontal derivative map (Figure 6), and the high in the Korazim Heights is the center of the elevation in the Bouguer anomaly map (Figure 5). Dotted lines are crests of the maximum gravity gradients. Hatched areas mark fault zones observed in seismic lines [after *Rotstein and Bartov, 1989; Rotstein et al., 1992*]. North of the Sea of Galilee, the barbed line marks the surface trace of a reversed fault which dips under the Korazim Heights. Arrows in the Korazim Heights and the eastern Galilee mark rotations [after *Ron et al., 1984; Heimann and Ron, 1993*].

the eastern margin probably does not extend north of latitude 32°49'N. Otherwise, a pull-apart basin should exist in the Bu-teikha Valley (Figure 1a), because the location of the left-lateral transform north of the lake is shifted to the left compared with the fault along the eastern margin of the lake. Seismic reflection profiles and gravity data north of the lake do not show the existence of a pull-apart basin there. Strike-slip motion thus is taking place along the eastern margin of the Kinarot Valley and the southern part of the eastern margin of the lake, while in the west, strike-slip motion is probably taking place along a boundary fault that extends from the western margin of the Kinarot Valley northward into the southern part of the lake. The western fault does not extend through the entire length of the lake, unlike an earlier suggestion that was based on gravity data from around the lake [Kashai and Croker, 1987].

Synthesis

The Sea of Galilee basin is divided into two distinct units. The southern half forms a continuation of the Kinarot Valley. The northern half was probably formed by two sets of faults, the N-S trending Dead Sea rift and the NW-SE to E-W trending eastern Galilee branching faults (Figures 3 and 8). The branching faults break the regions adjacent to the transform in the Sea of Galilee area [Ben-Avraham et al., 1980]. As a result, two subbasins with different trends were formed and superimposed within the area covered by the lake. The southern basin is probably a pull-apart which was formed as a result of the transform motion. The deepest part of this basin is located well south of the deepest bathymetric depression, which is probably a young feature that is actively subsiding now. The center of the bathymetric depression is located in the northern basin which was formed by a complex deformation, and it is not a pull-apart. The existence of the two units gives the lake its unusual shape, which is quite different from a typical rhomb-shaped basin.

In the north the Hula is a classical pull-apart basin with a left stepping jog occurring around latitude 33°06'N. The two faults may overlap by as much as 5 km and are separated by 6–7 km. The eastern fault extends from the Sea of Galilee northward parallel to the Jordan River gorge (the Jordan fault [Belitzky, 1987]). At the south margin of the Hula basin the strike-slip motion is probably shifted to the western boundary fault [Rotstein and Bartov, 1989]. The eastern boundary fault along the eastern margin of the Hula basin is mainly a normal fault. The gravity anomaly delineates the spatial dimensions of the basin to be 20 km by 6 km (Figure 5a). Drilling at the Notera 3 well in the Hula basin shows a sediment thickness of ~2.8 km [Heimann and Steinitz 1989]. The negative gravity anomaly associated with the basin is about 25 mGal, which gives an average sediment density of 2150 kg/m³. The sediment composition as revealed in the drill hole consists of alternating basalt and layers of peat, lignite, marl, sand, freshwater limestone, and conglomerate [Heimann and Steinitz, 1989].

South of the Hula pull-apart basin is the Korazim Heights block. Heimann and Ron [1993] inferred 11° counterclockwise rotation of this block from paleomagnetic data. They attribute the uplift of this block to a compression component which was introduced by a secondary strand of the Dead Sea transform (the Almagor fault) which strikes 020°, while the main strand of the transform (the Jordan fault) trends north-south (Figure 3). Rotstein and Bartov [1989] suggested that the Korazim Height is a "push-up" structure. They reasoned that if the

Jordan fault extends from the western side of the Sea of Galilee to the eastern side of the Hula Valley, then the fault trace is oblique to the direction of plate motion, which will result in shortening.

Seismic reflection data [Rotstein and Bartov, 1989] show that the main strike-slip fault east of the Korazim block dips westward at about 70° and present structural evidence for compression across the fault. The Jordan fault plane at a depth of 4–5 km lies beneath the surface trace of the Almagor fault; thus the Almagor fault is probably a secondary antithetic fault. We suggest that compression across the fault and the uplift of the Korazim Heights is the result of block rotation on the inclined Jordan fault. There can be two reasons for the shortening. First, if the uplifted block consists of NW-SE elongated slivers [Heimann and Ron, 1993], the slivers must undergo shortening during counterclockwise rotation. Second, rotation over an inclined fault surface, particularly when the fault surface decreases in dip to the north [Rotstein and Bartov, 1989], will force the edge of the block to climb the fault surface in order to fit the smaller available space. Therefore we interpret the uplift of the Korazim block not as a push-up structure but as a result of shortening forced by the rotation of the block.

A key kinematic question is the continuity of motion along the different segments of the Dead Sea transform in the area. Although a gradual right step from the western boundary fault of the Sea of Galilee to the southeastern part of the Hula Valley [Rotstein and Bartov, 1989] is a simple solution to this question, it will lead to an uplift centered around the right step. In other words, the uplift will be centered in the northern part of the Sea of Galilee, an area currently under subsidence. On the other hand, if the majority of motion along the Dead Sea transform is taken on the eastern boundary fault of the Sea of Galilee, then a small left step northward toward the Jordan fault is expected to create a small pull-apart basin. Seismic reflection [Rotstein and Bartov, 1989] and our gravity data do not support the existence of a basin under the NE shore of the Sea of Galilee. Hence we are forced to conclude that the motion in the northern Sea of Galilee is accommodated by either nonrigid deformation (e.g., crushed zone [Sibson, 1985]) or block rotations and numerous oblique and perpendicular normal faults (Figure 8).

A possible by-product of the counterclockwise rotation is opening along the northern coast of the Sea of Galilee, as suggested by the gravity data. The gravity map shows gradual increase in the gravity values toward the central and southern parts of the Sea of Galilee. This indicates that the northern Sea of Galilee gradually deepens southeastward. Large-scale counterclockwise rotations (53°) of Miocene rocks were also observed west of the lake (Tiberias province [Ron et al., 1984]). These rotations could result in opening of the Ginosar Valley northwest of the lake. The structure of the northern part of the lake is probably further complicated by a NW-SE trending normal fault system which terminates eastward in the lake. Thus the Sea of Galilee basin is perceived as a composite depression caused by a possible combination of pull-apart opening, rotational opening, and transverse normal faults.

Conclusions

The results of the gravity analysis over and around the Sea of Galilee indicate that two subbasins exist within the lake. The southern subbasin was formed as a pull-apart and is bordered on its east and west sides by segments of the Dead Sea trans-

form. This is the deeper subbasin with more than 6 km of sediments. The northern subbasin is bathymetrically the deepest. It is probably the most actively subsiding area in the Sea of Galilee and was probably formed as a result of the counterclockwise rotation of the Korazim block north of the Sea of Galilee and by branching faults.

Thus the Sea of Galilee is a composite depression that was formed by a possible combination of pull-apart opening, rotational opening, and transverse normal faults. We suggest that the structural complexity that led to the existence of two subbasins within the relative small area of the Sea of Galilee is the result of the breakup of coherent plates in front of the plate collision zone to the north.

Acknowledgments. This study was supported by the Earth Sciences Administration, Israel Ministry of Energy and Infrastructure and by the Dead Sea Research Center, Tel Aviv University. We thank Y. Rotstein for permission to publish the land gravity data; G. Amit and A. Golan for their help in obtaining and reducing the navigation data; N. Schoenberg and the Institute of Petroleum Research and Geophysics, Israel, for measurements of the tie-in gravity station; M. Ribakov for the use of his two-dimensional gravity modeling program; J. Zwinakis and O. Paran for drafting many of the figures; and the captain of R/V *Hermona* and the staff of the Kinneret Limnological Laboratory, Israel Oceanographic and Limnological Research Ltd. for their technical assistance. We also thank K. Klitgord for helpful discussions and D. Hutchinson and W. P. Dillon for their comments on the manuscript. JGR reviewers R. Jachens and J. Mechie and JGR Associate Editor G. R. Keller Jr. provided constructive criticism that greatly improved the manuscript.

References

- Bell, R. E., and A. B. Watts, Evaluation of the BGM-3 sea gravity meter system onboard R/V *Conrad*, *Geophysics*, *51*, 1480–1493, 1986.
- Belitzky, S., Tectonics of the Korazim saddle (in Hebrew with English abstract), M.S. thesis, 94 pp., Hebrew Univ., Jerusalem, Israel, 1987.
- Ben-Avraham, Z., Structural framework of the Gulf of Elat (Aqaba), northern Red Sea, *J. Geophys. Res.*, *90*, 703–726, 1985.
- Ben-Avraham, Z., Development of asymmetric basins along continental transform faults, *Tectonophysics*, *215*, 209–220, 1992.
- Ben-Avraham, Z., and U. S. ten Brink, Transverse faults and segmentation of basins within the Dead Sea Rift, *J. Afr. Earth Sci.*, *8*, 603–616, 1989.
- Ben-Avraham, Z., and M. D. Zoback, Transform-normal extension and symmetric basin: An alternative to pull-apart models, *Geology*, *20*, 423–426, 1992.
- Ben-Avraham, Z., R. Hanel, and H. Villinger, Heat flow through the Dead Sea rift, *Mar. Geol.*, *28*, 253–269, 1978.
- Ben-Avraham, Z., Y. Shoham, E. Klein, H. Michelson, and C. Serruya, Magnetic survey of Lake Kinneret-Central Jordan Valley, Israel, *Mar. Geophys. Res.*, *4*, 257–276, 1980.
- Ben-Avraham, Z., A. Ginzburg, and Z. Yuval, Seismic reflection and refraction investigations of Lake Kinneret-Central Jordan Valley, Israel, *Tectonophysics*, *80*, 165–181, 1981.
- Ben-Avraham, Z., G. Shaliv, and A. Nur, Acoustic reflectivity and shallow sedimentary structure in the Sea of Galilee, Jordan Valley, *Mar. Geol.*, *70*, 175–189, 1986.
- Ben-Avraham, Z., G. Amit, A. Golan, and Z. B. Begin, The bathymetry of Lake Kinneret and its structural significance, *Isr. J. Earth Sci.*, *39*, 77–84, 1990.
- Ben-Menahem, A., A. Nur, and M. Vered, Tectonics, seismicity and structure of the Afro-Eurasian junction—The breaking incoherent plate, *Phys. Earth Planet. Inter.*, *12*, 1–50, 1976.
- Folkman, Y., Magnetic and gravity investigations of the crustal structure in Israel (in Hebrew), Ph. D. thesis, Tel Aviv Univ., Tel Aviv, Israel, 1976.
- Freund, R., A model of the structural development of Israel and adjacent areas since Upper Cretaceous times, *Geol. Mag.*, *102*, 189–205, 1965.
- Freund, R., The concept of the sinistral megashear, in *Lake Kinneret, Biogr. Biol.*, vol. 32, edited by C. Serruya, pp. 27–31, Junk, The Hague, 1978.
- Garfunkel, Z., Internal structure of the Dead Sea leaky transform (rift) in relation to plate kinematics, *Tectonophysics*, *80*, 81–108, 1981.
- Ginzburg, A., and Z. Ben-Avraham, Structure of the Sea of Galilee graben, Israel, from magnetic measurements, *Tectonophysics*, *126*, 153–164, 1986.
- Ginzburg, A., J. Makris, K. Fuchs, C. Prodehl, W. Kaminski, and U. Amitai, A seismic study of the crust and upper mantle of the Jordan-Dead Sea rift and their transition toward the Mediterranean Sea, *J. Geophys. Res.*, *84*, 1569–1582, 1979.
- Girdler, R. W., The Dead Sea transform fault system, *Tectonophysics*, *180*, 1–13, 1990.
- Heimann, A., and H. Ron, Geometric changes of plate boundaries along part of the northern Dead Sea transform: Geochronologic and paleomagnetic evidence, *Tectonics*, *12*, 477–491, 1993.
- Heimann, A., and G. Steinitz, $^{40}\text{Ar}/^{39}\text{Ar}$ total gas ages from Notera #3 well, Hula Valley, Dead Sea rift: Stratigraphic and tectonic implications, *Isr. J. Earth Sci.*, *38*, 173–184, 1989.
- Kashai, E. L., and P. F. Croker, Structural geometry and evolution of the Dead Sea-Jordan rift system as deduced from new subsurface data, *Tectonophysics*, *141*, 33–60, 1987.
- Marcus, E., and J. Slager, The sedimentary-magmatic sequence of the Zemah-1 well (Jordan-Dead Sea rift, Israel) and its emplacement in time and space, *Isr. J. Earth Sci.*, *34*, 1–10, 1985.
- Mor, D., The volcanism of the Golan Heights (in Hebrew with English abstract), Ph.D. thesis, 159 pp., Hebrew Univ., Jerusalem, Israel, 1986.
- Neev, D., *The geology of Lake Kinneret. Kinneret—Assemblage of Scientific Articles*, (in Hebrew), 114 pp., Publ. Lake Kinneret Auto., Tzemak, Israel, 1978.
- Nur, A., and Z. Ben-Avraham, The Eastern Mediterranean and the Levant: Tectonics of continental collision, *Tectonophysics*, *46*, 297–312, 1978.
- Picard, L., and U. Golani, Geological map of Israel, scale 1:250,000, northern sheet, Govt. Printer, Jerusalem, Israel, 1976.
- Ron, H., R. Freund, Z. Garfunkel, and A. Nur, Block rotation by strike-slip faulting: Structural and paleomagnetic evidence, *J. Geophys. Res.*, *89*, 6256–6270, 1984.
- Rotstein, Y., and Y. Bartov, Seismic reflection across a continental transform: An example from a convergent segment of the Dead Sea rift, *J. Geophys. Res.*, *94*, 2902–2912, 1989.
- Rotstein, Y., Y. Bartov, and U. Friesslander, Evidence for local shifting of the main fault and changes in the structural setting, Kinarot basin, Dead Sea transform, *Geology*, *20*, 251–254, 1992.
- Schulman, N., The geology of the central Jordan Valley (in Hebrew, English abstract), Ph.D. thesis, Hebrew Univ., Jerusalem, Israel, 1962.
- Sibson, R. H., Stopping of earthquake ruptures at dilatational fault jogs, *Nature*, *316*, 248–251, 1985.
- ten Brink, U. S., N. Schoenberg, R. L. Kovach, and Z. Ben-Avraham, Uplift and a possible Moho offset across the Dead Sea transform, *Tectonophysics*, *180*, 71–85, 1990.
- ten Brink, U. S., Z. Ben-Avraham, R. E. Bell, M. Hassouneh, D. F. Coleman, G. Andreasen, G. Tibor, and B. Coakley, Structure of the Dead Sea pull-apart basin from gravity, *J. Geophys. Res.*, *98*, 21,877–21,894, 1993.
- van Eck, T., and A. Hofstetter, Fault geometry and spatial clustering of microearthquakes along the Dead Sea—Jordan rift fault zone, *Tectonophysics*, *180*, 15–27, 1990.
- Walley, C. D., A braided strike-slip model for the northern continuation of the Dead Sea Fault and its implications for Levantine tectonics, *Tectonophysics*, *145*, 63–72, 1988.
- Z. Ben-Avraham, Department of Geophysics and Planetary Sciences, Tel Aviv University, Tel Aviv, 69978, Israel. (e-mail: zri@jupiter1.tau.ac.il)
- R. Bell, Lamont-Doherty Earth Observatory, Palisades, NY 10964.
- M. Reznikov, Institute for Petroleum Research and Geophysics, P. O. Box 2286, Holon 58122, Israel.
- U. ten Brink, U.S. Geological Survey, Woods Hole, MA 02543.

(Received November 9, 1994; revised September 25, 1995; accepted September 26, 1995.)